fibers

MDPI

Review

Corrosion Behavior of Fiber-Reinforced Concrete—A Review

Ganesh Naidu Gopu and Sofi Androse Joseph *

Department of Structural and Geotechnical Engineering, School of Civil Engineering, Vellore Institute of Technology, Vellore 632014, Tamil Nadu, India; ganeshnaidu.gopu2016@vitstudent.ac.in
* Correspondence: asofi@vit.ac.in or sofime@gmail.com

Abstract: Corrosion study of conventional reinforcement in concrete has been accorded wider importance in the last few decades based on the losses occurring in monitoring concrete structures. It is well known that the presence of chloride ions is one of the most significant factors contributing to the corrosion of reinforcing steel. Practically, it is observed that in the marine environment, the activating substances such as chlorides that penetrate the steel can counteract the passivity locally when the electrolyte is highly alkaline. The concrete cover is changed chemically when chloride ionspenetrate into the material, whereupon the pore solution is neutralized. Based on numerous studies, it is evident that steel fibers and glass fibers have less impact on cracked sections in a chloride environment and can oppose chloride infiltration. Glass fibers, when exposed to repeated freeze and thaw conditions, protect the passive layer. This review article highlights the corrosion behavior of reinforced concrete involving various factors such as cracking behavior, transportation, electric conductivity, resistivity, and diffusion of chloride ions in the presence of steel and glass fibers.

Keywords: corrosion; chloride; glass fibers; reinforced concrete; steel fibers

check for updates

Citation: Naidu Gopu, G.; Joseph, S.A. Corrosion Behavior of Fiber-Reinforced Concrete—A Review. *Fibers* **2022**, *10*, 38. https://doi.org/10.3390/fib10050038

Academic Editor: Doo-Yeol Yoo

Received: 8 February 2022
Accepted: 13 April 2022
Published: 21 April 2022

Publisher's Note: MDPI stays neutral with regard to jurisdictional claims in published maps and institutional affiliations.

1. Introduction

Reinforced concrete structures are designed to withstand heavy loads even over long durations of time [1]. However, one of the most common phenomena that can adversely affect the durability of concrete is corrosion [2]. The two major reasons that generally lead to corrosion when reinforced concrete is exposed to the marine environment are carbonation and chloride attack [3]. The rate of corrosion in the propagation period can be described by the relative humidity in the concrete and the mean temperature of the structure [4]. About 18% of total service life can be expected in concrete flexural members in which corrosion-induced concrete cracking occurs when subjected to a marine environment. In addition, due to corrosion-induced excessive deflection, flexural members become unserviceable. Chloride ions attack the concrete surface, and due to the repeated wetting and drying mechanism, chloride ions are dispersed into the surface, reducing the alkalinity of the pore water, and ferrous oxides tend to form pits on the reinforcement [4]. Pitting corrosion further leads to the spalling of concrete and leads to the formation of cracks on the surface of the concrete. The slow process of crack width expansion results in the deterioration of concrete structures [5]. In the marine environment, transportation of chloride ions proceeds in the order of capillary suction, absorption, permeation, and diffusion until local depassivation occurs [6]. Many researchers report that the capillary suction mechanism is a major source of chloride ions entering concrete, especially in the case of saturated concrete [7–13]. The thickness of the concrete cover that is exposed to the water surface has an adverse effect on the capillary suction and the highest values of chloride ion presence are found just above the water surface In water that contains chloride, chloride ingress is accelerated by repeated wetting and drying of the concrete [14]. Chloride values must be above the critical threshold value that depends on concrete cover and moisture content to reduce corrosion at the rebar level [15]. The chloride resistance should be improved upon for the concrete and passive film on the reinforcement to resist electrochemical reactions and to control the corrosion process [16]. The effect of chloride ions on steel corrosion in concrete is kinetic rather than thermodynamic. The passive coating is broken down by chloride ions, and corrosion continues without further chloride effect, according to a simplified perspective [17]. Fibers were added to conventional concrete to improve the mechanical properties in controlling the corrosion characteristics such as crack formation [18]. Over certain periods of time, fibers were increasingly introduced in pavements, slabs, and many structural components due to their extensive advantages [19]. The inclusion of fibers is considered the most effective technique for controlling corrosion and reducing chloride ion diffusion. Kakooei et al. mentioned that the presence of fibers in concrete reduced permeation and concrete cracking [20]. Further, the length and properties of fibers also have an impact on controlling corrosion to a large extent [21]. The bond–slip behavior in concrete also tends to show an significant change in the presence of fibers [22]. The different types of fibers are shown in Figure 1.

Figure 1. Types of fibers [23].

This literature review focuses on the impact of steel and glass fibers on the process of chloride-induced corrosion. Data from experimentation and published research on steel and glass fibers in concrete have been analyzed.

2. Effect of Fibers on Concrete Cracking Behavior

Early research on fiber-reinforced concrete (FRC) focusing on adopting short-length fibers in concrete to test the tensile strength and to control effective cracking [24] has been highlighted. The need to continue the research on the study of mechanical properties and fracture characteristics of concrete has been discussed in detail. According to Furlan et al. [25], beams with fibers have a closely packed cracking pattern which has the same pattern of failure when compared with beams. The addition of 2% fiber to the concrete can reduce the intense diagonal cracking of the beam. Figure 2 shows the types of failures that a beam can undergo for different quantities of fiber content. Fracture parameters such as fracture energy and toughness can affect the crack behavior during the addition of fibers, even at very low volumes, as shown in Figure 3 [26]. As per the study by Lim et al. [27], beams with steel fibers under four-point loading exhibited a failure mode from shear to flexure with an increase in fiber content, resulting in the elimination of spalling of concrete during the post-cracking stage by holding the matrix together. Thus, an optimal amount of steel fiber matrix can result in a reduction in stirrups and control shear cracking.

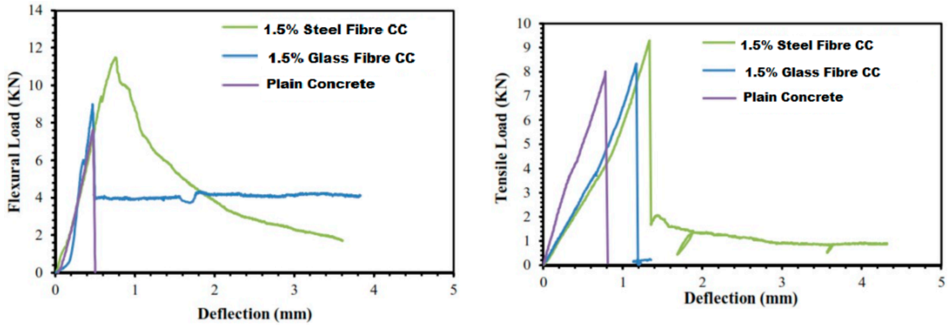

Figure 2. Failure type based on the quantity of fibers [28].

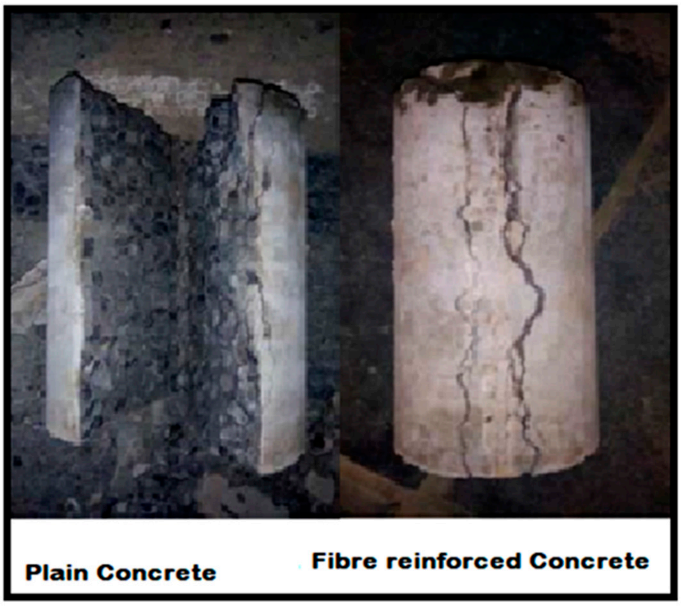

Figure 3. Crack behavior of plain concrete and fiber-reinforced concrete [29].

In a study by Bernardino et al. [30], fiber-reinforced concrete containing steel and polypropylene fibers was tested for failure and a load–deflection curve was generated. It was found that under flexure, load–deflection and load crack mouth opening exhibited a linear variation. In another study by Qi et al. [31], the plastic shrinkage cracking response of fiber-reinforced concrete was analyzed using image analysis. The study states that when the fiber volume increases, the plastic shrinkage cracking width is reduced, and further, the size of the fiber can also affect the crack width [32]. Many studies are in agreement that the presence of fiber content in concrete can resist cracking and can also reduce the crack width. With the increase in fiber volume, the failure mode of the concrete changes from shear to flexure, resulting in an increase in the crack formation time [33–39]. The mechanisms of cracking in concrete materials have posed a constant challenge, and we have not yet attained a reasonable level of understanding of these mechanisms. Because cementitious materials are complicated, this lack of understanding is due to the lack of knowledge on the subject. As a result of its unique ability to capture fracture energy in real time, acoustic emission (AE) monitoring has been attracting growing interest over the last few decades. As a result of an aging and failing civil infrastructure network throughout the world, this has occurred. As seismology-based AE methods for monitoring and characterizing cracking mechanisms in concrete structures, the qualitative b-value analysis and the quantitative moment tensor inversion (MTI) approaches are introduced by Mhamdi [40].

3. Impact of Fibers on Electric Resistivity

One of the major techniques that have been developed for the corrosion assessment of reinforced concrete is electric resistivity. The ratio of the applied potential difference to the current produced is the electrical resistivity. A cell constant is multiplied by the value. The resistivity of a substance varies substantially depending on its properties. The geometric ties of a material have no effect on its resistivity. Standard testing procedures and equipment are used to determine electrical resistance in practical situations [41]. The electrical resistivity of the material is computed by multiplying the obtained value by the cell constant. The cell constant depends on the testing apparatus. The two factors that influence the electrical properties of concrete are chloride ingress and moisture. Resistivity is usually expressed in ohm-meters (ohm m). Intrinsic factors that influence the electric resistivity are porosity, water-to-cement ratio, quality of aggregate, and pozzolanic material used [42]. Moisture and chloride contamination can alter the electrical resistivity of concrete. The change in electrical resistivity with increasing moisture content was markedly decreased after a particular moisture level was attained, indicating a lesser symptom. Furthermore, the electrical resistance of concrete contaminated with more than 19.2 kg/m^3 of chloride ions by weight of concrete does not change with moisture content, showing that high chloride concentrations can considerably accelerate the reinforcement corrosion even in near-dry concrete [43]. Usually, corrosion is formed due to electrochemical reactions, and the rate of influence may vary depending on the electric resistivity of the concrete. On any structure, the electrical surface resistivity of concrete can be tested nondestructively. The resistance is measured by placing electrodes on the surface, and the resistivity may be computed using cell geometry. Low resistivity is generally associated with a significant risk of corrosion [44]. In a study by Lakshminarayanan et al. [45], the galvanostatic charging approach was used to determine concrete resistivity, which was proposed and tested for a variety of concrete mix proportions and cover thicknesses. The resistivity varies as a hyperbolic function of the amount of curing days, according to their findings.

Sbartaï et al. [46] have demonstrated a radar direct wave technique to assess the correlation of electric resistivity with physical conditions of concrete, and the technique has shown that radar wave signals are highly affected by the moisture content and chloride ingress, which in turn affects electric resistivity, increasing the corrosion of reinforcement in concrete. In accordance with the experimental link between diffusivity and resistivity, the electrical resistivity of concrete can be used as a durability indicator, as well as for quality control and rapid classification of concrete. Resistance measures, when combined with chloride diffusivity readings, can be used to indirectly modify chloride diffusivity. It is important to emphasize that the association was found for saturated specimens at a temperature of 20 °C. The changes in moisture levels and temperature could culminate in incorrect results [47]. Electrical resistivity measurement for concrete materials shows potential as a quality control and performance assessment tool. If the necessary geometry variables are applied, both the uniaxial and Wenner probe approaches produce reliable results. The uniaxial approach is useful for assessing concrete samples or drilled cores, but the Wenner probe method is preferable for on-site evaluation. Changes in the temperature and characteristics of the pore solution during the rapid chloride penetration (RCP) test are mostly responsible for the nonlinear relationship between electrical resistivity and RCP values. For quantification, a link between electrical resistivity and diffusion coefficient would be more acceptable [48]. A typical test setup for the electric resistivity is shown in Figure 4.

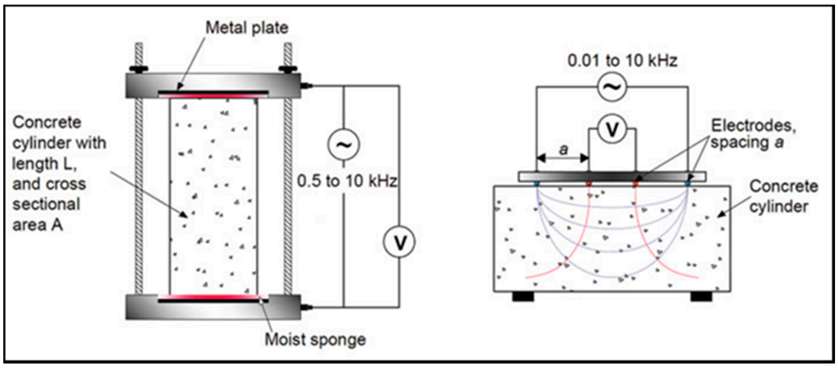

Figure 4. Typical electric resistivity setup, image sourced from [49].

4. Chloride Ion Diffusion in Cracked and Uncracked Concrete

It is presumed that the capillary porosity of uncracked concrete is responsible for chloride ion diffusion. Diffusion decreases as the w/c ratio decreases and the cement is totally hydrated in concrete. In contrast, cracks in concrete have the potential to significantly alter the diffusion coefficient. Many researchers have suggested that numerous parameters such as crack width, crack depth, and atmospheric conditions have an impact on the diffusion of concrete. This has been proven through observations [50]. As previously indicated, problems related to chloride penetration may be enhanced in the presence of cracks, which is a burden in any case. The results of these experiments will be presented in this section, which will be of great interest to investigators of reinforced concrete under the combined effects of cracking and chloride ingress, as illustrated in Figure 5.

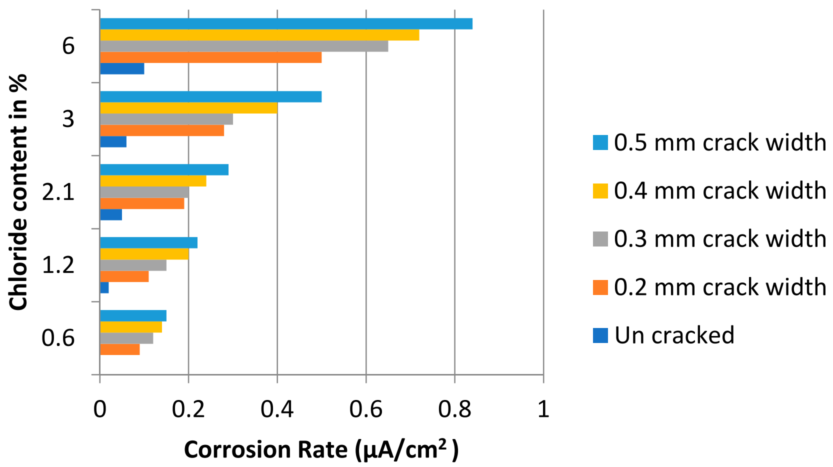

Figure 5. Average chloride concentration in concrete influenced by crack quantity [31,51,52].

Researchers conducted an electron probe microanalysis on a chloride-exposed specimen to determine the penetration depth and chloride ion concentration. They concluded that increasing the water-to-cement (w/c) ratio results in a higher penetration rate of Cl^- ions, not only from the exposed surface but also from the area surrounding the cracks as well as from the exposed surface itself. For the most part, the penetration depth of the fracture surface is equal to or slightly greater than the penetration depth of the exposed surface, especially at higher w/c values of 0.45 and 0.65, according to conventional wisdom [51]. According to Kobayashi et al. [52], the chloride proofing of concrete with fine cracks can be improved with a reduced w/c ratio and desirable fiber content. Hansson et al. [53], in their study of chloride ion penetration in a cracked beam using different types of cement, have concluded that steel that is protected beneath the high-performance concrete (HPC) from macrocell and microcell corrosion compared to ordinary Portland cement concrete (OPCC). LPR test results have shown that the current density of HPC is 3 times lower than that of OPCC. An increase in cement content can decrease the mean penetration depth of chloride ions as chloride ions can bind to the cement matrix [54]. In the accelerated migration test, the chloride diffusion coefficient in cracked concrete and its relationship with crack width are determined [55]. In half-cell potential testing, increases in crack width have a nonlinear relationship with the corrosion length on implanted steel, but a versatile agreement between local and field investigations is still needed [56].

In a study by Ye et al. [57], a simplified method other than Fick's second law is defined to determine the chloride content in concrete, and the method explains the relationship between the crack width, crack pattern, and interface of the transition zone of the aggregates and the cement. An equation was proposed to define the chloride diffusion coefficient. The steel–concrete interface can change the cast steel behavior under loading to act as passive or active for the same concrete covers, and the chloride diffusion coefficient can also affect the severity of the exposure environment [58]. In a study by Otieno et al. [59], parallel experiments were conducted, and the corrosion behavior of concrete in the marine environment was identified by keeping one variable constant and interchanging the remaining variables. This research summarizes that corrosion rate increases with a considerable quality of the binder and a desirable water-to-cement ratio along with the severity of the exposure environment. The chloride ion diffusion techniques are mentioned in Figure 6.

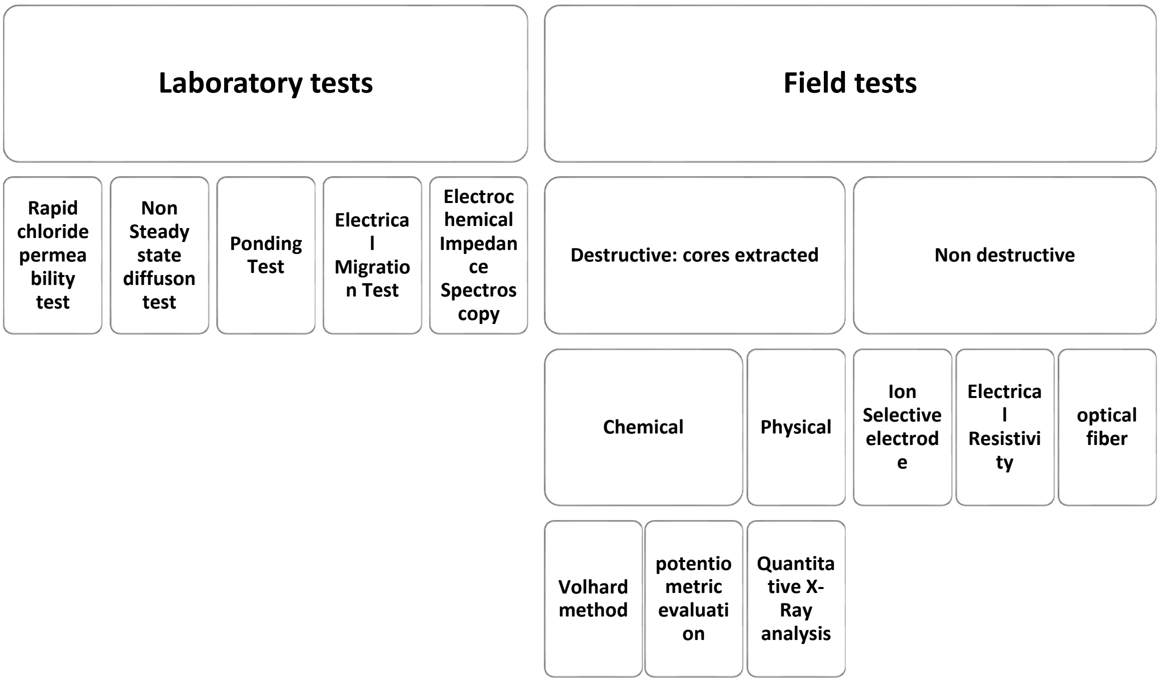

Figure 6. Chloride ionmeasurement techniques [4,53,60–66].

Impact of Fibers on Chloride ion Diffusion in Cracked Concrete and Uncracked Concrete

In an earlier study of chloride ion diffusion in fiber-reinforced concrete by Mangat and Guruswamy (1987) [67], uncracked and flexural cracked specimens were tested in the laboratory and in the marine tidal environment to measure the chloride ingress of the embedded steel in the concrete for a duration of 1250 days. The research found that the fibers in the concrete have an impact on the crack width, which reduces the chloride ion penetration into the concrete. ElMaaddawy (2006) [68] investigated concrete corrosion activity and chloride-induced cracking of concrete using fiber-reinforced polymer (FRP) wraps. Cylindrical specimens were tested under an accelerated corrosion test, and applied potential and wrapping and unwrapping of the FRP were taken as test variables. Parameters determining chloride and corrosion severity were measured; the mass loss of steel and circumferential expansion were also measured. The test results revealed that FRP wrap inclusion decreased current, mass loss, and circumferential expansion compared to unwrapped specimens and reduced the risk of corrosion. The research is in agreement with a work by Soudki (2007) [69], in which CFRP laminates were introduced to reduce the chloride ion diffusion. Another study, by Banthia (2007) [70], which has concentrated on enhancing the durability of concrete by introducing fibers has stated that fiber introduction can reduce the shrinkage cracks and permeability of concrete, which can increase the life and serviceability of the concrete.

Abbas et al. [71] recommended a rapid chlorine migration test (ASTM C1202-10) to assess the chloride resistance of uncracked fiber-reinforced concrete specimens. It was also necessary to utilize Fick's second rule in order to obtain the chloride diffusion coefficient. Both the chloride diffusion coefficient and the charge of the FRC samples were found to be lower than those of the RC samples in this study. This was attributed to FRC's ability to control microfractures during curing and handling, which was made possible by the presence of fibers [72]. In general, fiber reinforcement retards the start of reinforcement corrosion-induced cracking [73,74]. The fiber–matrix interface may be critical in this process, resulting in uncracked FRC. In general, fiber matrix lowers the corrosion expansion in steel bars. As a result, the fiber–matrix contact is considered to be denser and more uniform than the interface between normal steel rebars and the matrix, hence preventing hazardous solutes from entering the fiber-reinforced concrete (FRC) [75]. If a significant amount of calcium hydroxide exists at the fiber–matrix contact, it is possible that chloride binding will be enhanced. Significant damage at the fiber–matrix contact would result in a progressive and localized decrease in the cross-section of the fiber as a result of corrosion. Sahmaran (2007) [76], in his study on the transportation mechanism of chloride ions in engineering cementations composites (ECCs), used 2% fiber content and employed salt ponding, i.e., immersion of the specimen in the NaCl solution, as a testing method. Research reveals that ECC specimens tend to reduce chloride diffusivity, due to the presence of a tight cracking pattern. Another study by Sahmaran (2009) [77] evaluates the durability performance of microcracked ECCs. Microcrack introduction caused capillary suction of water and chloride ion diffusion. Bhargava (2008) [78], in his study, investigated the permeability of fiber-reinforced concrete, adopted a method of applying compressive stress on the specimen, and predicted models for the permeability coefficient and chloride diffusion coefficient. According to the findings of the research, when compared to plain reinforced concrete, fiber-reinforced concrete under compression demonstrates a reduced permeability up to a certain threshold value. When the permeability of plain concrete exceeds a certain threshold value, it grows at a faster rate than that of fiber-reinforced concrete. Kakooei et al. [20] introduced polypropylene fibers in concrete and investigated the corrosion characteristics. Apart from improving corrosion resistance, the presence of polypropylene fibers minimized the permeability, volumetric expansion, and contraction of concrete, reducing the probability of cracking. Liu et al. [79] conducted research on calculating the chloride ion diffusion in glass- and polypropylene-fiber-reinforced concrete by establishing a model considering the interfacial transition zone of aggregates and voids due to fiber addition. The diffusion coefficient of concrete with glass fiber is lower than that of concrete with polypropylene fibers and a combined fiber matrix. Soylev [80] studied the durability of concrete with low-volume glass, polypropylene, and steel fibers. Results show the long-term exposure of the glass and polypropylene fibers has a risk of chloride ion permeability compared to steel fibers at a 0.45 w/c ratio.

Akhavan (2013) [81] used electric impedance spectroscopy (EIS) to evaluate the ion diffusivity of a cement matrix. Evaluated results and the theoretical justification indicate that the chloride diffusion coefficient has no direct relationship with the crack width and linearly changes with the volume fraction of cracks. Ramli et al. [82] studied the durability properties of concrete using coconut fibers, and experimental results from the study reveal that fiber introduction restrains crack development and can suppress chloride diffusion. The most optimal volume of fiber should not be more than 1.2% according to the study, and this may be due to the degradation of fibers. Berrocal [83] evaluated corrosion using the half-cell potential values for the cracked section with fibers. After 17 weeks of exposure, corrosion was severe, and crack width was monitored regularly. Niu (2019) [84] experimentally investigated the chloride permeability of basalt–polypropylene fiber reinforced concrete; the study reveals that fiber distribution in the concrete tends to form a three-dimensional system, and at low fractions (<0.15%), the chloride diffusion coefficient is reduced, reducing the formation of microcracks and capillary suction of pore water. This research is in line with study of Guo et al., where only basalt fibers were adopted. Finally the chloride diffusion coefficients of the FRC samples were found to be lower than those of RC samples.

5. Chloride-Induced Corrosion of Fibers Incorporated in Reinforced Concrete (RC)

In general, concrete deterioration can be attributed to a range of physical, chemical, or mechanical processes that frequently act in concrete [85]. Corrosion of steel reinforcement is one of the most common deterioration mechanisms that occur in reinforced concrete structures and structures made of steel. During an electrochemical reaction, charge is transferred from the anode to the cathode, resulting in corrosion. An effective passive coating protects steel surfaces from corrosion when they are exposed to the alkaline environment of hydrated concrete in the majority of situations [86,87]. However, due to chloride infiltration or carbonation, this passive coating might deteriorate, resulting in active corrosion, as shown in Figure 7.

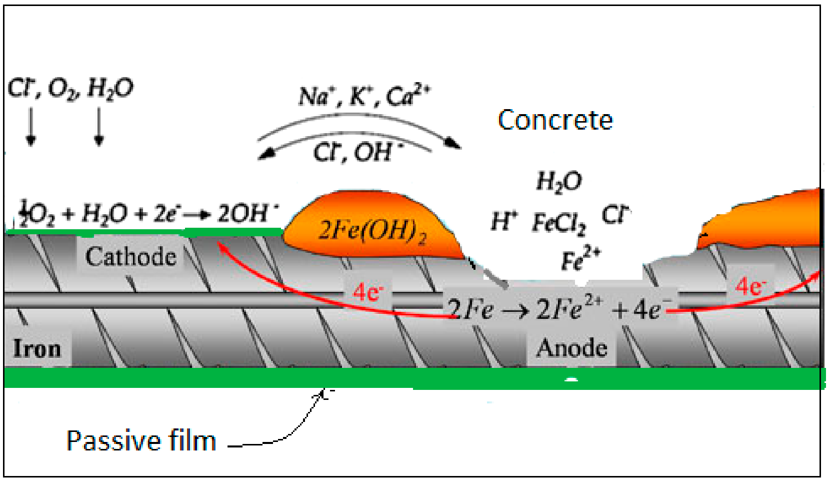

Figure 7. Corrosion of steel bar in concrete [88–90].

Because corrosion occurs in two unique phases, it can be examined in terms of two phases: the corrosion initiation phase and the corrosion propagation phase. Typically, the initiation phase refers to the amount of time it takes for external aggressors to start their attacks. As a result of the penetration of the reinforcing steel into the concrete, the steel will become depassivated. Steel reinforcement is corroded during the propagation phase, reducing the structural integrity and making the structure less safe. Figure 8 shows the service life of a structure as a function of its age, in accordance with the design of Tuutti [4].

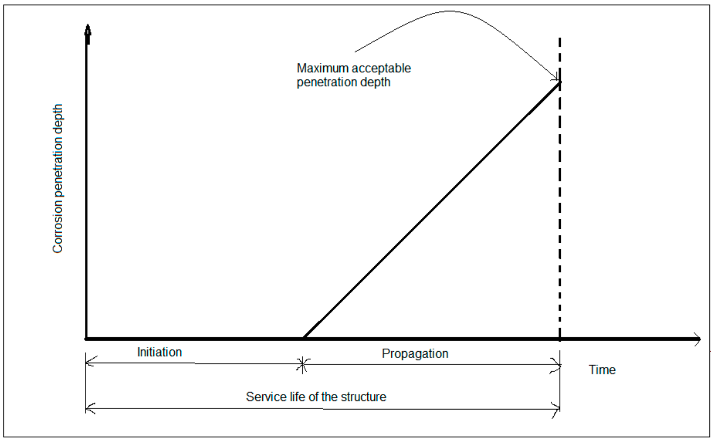

Figure 8. Tuutti's service life model [91].

Additionally, the existence of cracks has a significant effect on the corrosion process in concrete at both the start and propagation periods; given the fundamental difference between the cracking processes in FRCs and ordinary concrete, it is logical to assume that the deterioration mechanisms are similarly distinct [92]. Assuming that these fibers are particularly vulnerable to external agents, substantial degradation would be expected when exposed to harsh conditions. Fibers that were only a few millimeters deep showed evidence of corrosion, but those that were fully embedded in concrete remained undamaged. This has been validated and documented by various researchers [93–98]. Furthermore, substantial rust stains on the concrete surface are often accompanied by the corrosion of superficial fibers, which can be seen in some cases at an early age of exposure [99–102]. This could be a problem if steel fibers are to be used in concrete elements that will be on display for the whole of their service lifetime [103–105]. The depth at which fibers are rapidly corroded is generally less than 10 mm, as shown in Table 1, regardless of other parameters such as environmental abrasiveness and exposure period.

Table 1. Depths at which corrosion affects the fibers in the concrete.

W/C	Concrete Depth (mm)	Exposure Time	Details	Reference
0.46	1.6	5 years	0.2 kg/m^2 of NaCl applied once a week	Lankard et al. [106]
0.75	6.4	325 days	At the coastal ambient temperature, combined exposure	Hanant et al. [107]
0.60	3	12 months	Containing 35 g/L NaCl on a weekly basis	Granju et al. [108]
0.40	2	130 days	Experiment with a 10% NaCl aqueous solution	Corinaldesi et al. [72]
0.6	6.4	6 months	Flow device for specimens that are only half-submerged in seawater.	Rider et al. [109]
0.44	3.2	67 days	$CaCl_2$ salt solution that is 5% by weight in the fog chamber	Aitcin et al. [110]
0.78	1	7 months	Containing 35 g/L NaCl on a weekly basis	Balounch et al. [111]

It is critical to remember that the deterioration process in fiber-reinforced concrete (FRC) is significantly influenced by the type of fiber used. While steel fibers are unquestionably susceptible to corrosion, some researchers concluded that the presence of milliscale features on the surface of steel fibers increases their corrosion resistance [112]. After being subjected to a wide range of environmental conditions, including freshwater and marine environments, for periods ranging from 7 to 24 months, the durability of FRC reinforced with steel and macrosynthetic fibers was examined in pre-cracked specimens [112–114].

The synthetic fibers themselves have been shown to be exceptionally resilient in a variety of conditions, both freshwater and marine. With a crack diameter of 0.20 mm, corrosion caused significant damage to the steel fibers in the specimens tested. The formation of pits in the crack bridging zone of steel fibers, as well as deformed sections, results in a large reduction in the cross-section of the fibers, as well as a significant reduction in residual tensile strength. Additionally, some study has revealed that steel fibers coated with an inhibitor such as triethanolamine could be used to address the steel fiber corrosion issue in FRC, which could be beneficial [115,116]. Moreover, it has been discovered that FRC specimens composed of glass fibers with crack widths less than 0.1 mm are more corrosion-resistant in a marine environment [117]. The corrosion resistance of FRC was investigated in another study using two different types of fibers: glass fibers and low carbon steel fibers. After one year in the marine environment, glass-fiber-reinforced concrete (GFRC) demonstrated negligible corrosion, whereas low carbon steel reinforced concrete (LCSRC) exhibited significant corrosion [118]. The improved corrosion resistance of steel fibers and low carbon steel fibers may also be due to the zinc coating applied to their surfaces. It has been shown that corrosion of steel fibers in FRC can also increase their roughness, which can improve the frictional interaction between the fibers and the matrix, hence enhancing the residual tensile strength of the material [119–121]. In some cases, the structural performance of concrete samples has been employed as an indirect method of measuring the corrosion resistance of steel fibers. As a result, steel fiber reinforcement has been credited with a better level of corrosion resistance due to the absence of harmful effects on structural integrity after prolonged exposure to corrosive conditions, as noted by a large number of researchers [119–126]. However, conventional carbon-steel fibers break down when surface cracks appear. In a number of studies, a critical crack width has been said to be the point at which fibers flowing through the cracks cannot be corroded. This important crack width appears to be very dependent on the type of fiber used. On the other hand, Mangat and Gurusamy [127] investigated the long-term seawater sustainability of SFRC in both cracked and uncracked concrete specimens. For the experiment, the researchers used low carbon steel fibers and melt-extract steel fibers, and they recreated coastal conditions by spraying seawater on specimens in a curing chamber twice a day for 24 h. Low carbon steel and melt-extract steel fibers bridge the gaps of 0.24 and 0.94 mm width, and a small amount of corrosion was observed after 450 days of exposure to air and water. Nemegeer et al. [128] created 0.2 and 0.5 mm wide cracks in 100 mm cube specimens built of fiber-reinforced concrete (FRC) using low carbon and zinc-coated steel fibers. According to their findings, after 18 months, the greatest corrosion depth on the fibers was 16 mm in one localized area, and fracture widths up to 0.5 mm would have no detrimental effect on corrosion. Granju and Balouch [108] obtained equivalent findings by pre-cracking specimens in a three-point bending arrangement to create a crack mouth opening of 0.5 mm using a 100 $\times$ 100 $\times$ 500 mm specimen. The study concludes that even after a year of exposure to a hostile marine-like environment, specimens with cracks left open during the exposure period gained strength at both the peak and post-peak stages. Based on their findings, they concluded that the most reasonable explanation for this behavior was an improved link between the fibers and the concrete matrix as a result of the moderate corrosion that had been discovered on the fiber surfaces. With the exception of the zinc-coated fibers, the flexural behavior was observed to be embrittled in all the samples. Table 2 provides a concise overview of the influence of fibers on the corrosion of steel reinforcement in concrete.

Table 2. An overview of experimental investigations on the corrosion of rebar in fiber-reinforced concrete.

Type of Fiber (Aspect Ratio-Content (% Volume))	W/B	Exposure	Period	Pre-Cracking	Diameter/Cover Thickness	Phase Investigated	Effect	Authors
Glass (500-1.5) Steel (80-0.75)	Concrete 0.45 OPC	3% NaCl sol. + drying under 20 °C and 60% RH with 3V DC voltage cyclic wetting	52 weeks	No	12/25	Propagation	Positive	Mihashi et al. [111]
Steel (zinc-coated) (60-1.5)	Concrete 0.55 OPC	3 kg/m^3 NaCl mixed-in + 12-hour wet–dry cycles	6 months	No	10/25	Initiation	Positive	Someh and Saeki [129]
Steel (65-0.5)	Concrete 0.65 OPC	Cyclic ponding with 3.5% NaCl sol.	Not provided	Fixed load Sustained/Dynamic	14/25	Initiation Propagation	Unclear	Nis et al. [86]
Steel (50-4.5)	Mortar 0.45/0.55 OPC	Immersion in a solution of 3.5% NaCl with water	7 months	No	9.52/32.7	Initiation Propagation	Unclear Positive	Grubb et al. [130]
Glass fiber (1000-1.5)	Mortar 0.3/0.6 OPC	2 days of cyclic wetting in 3.1% NaCl solution + 5 days of drying at 60% RH	Not provided	Fixed load sustained	9/20	Propagation	Positive	Haraishi et al. [131]
Steel (57-1.0)	Concrete 0.65 OPC	3 days of cyclic immersion in 10% NaCl + air drying at 55% RH for 4 days	95 weeks	No	19/25	Initiation Propagation	None	Matsumoto et al. [37]
Steel (55-1.0) Glass (90-0.5) Polypropylene (45-0.75)	Concrete 0.44 OPC	16.5% NaCl sol for cyclic ponding for 2 weeks, then air drying for 2 more weeks	660 days	No	Not provided	Initiation Propagation	Unclear None	Kim et al. [132]
Carbon (330-0.35)	Concrete 0.5 Admixtures	Immersion in 0.5 N NaCl sol.	25 weeks	No	9.52/34.2	Initiation Propagation	Unclear Negative	Hou and Chung [133]
Glass fiber (530-0.1/0.3)	Concrete 0.55 OPC	3 days of cyclic immersion in 3.5% NaCl + air drying at 55% RH for 4 days	56 weeks	Fixed load Sustained	10/25	Initiation Propagation	Positive	Sappakittiparkorn et al. [134]
Steel (80-1.0) PVA (300-1.5)	Concrete 0.45 OPC + FA	3.5 days of cyclic wetting in a % NaCl sol. + 8V DC drying	141 days	No	16/52	Propagation	Positive	Maalej et al. [135]
Polyethylene (500-1.5) Basalt fiber (80-1.5)	Mortar 0.45 OPC + SF	% NaCl sol. + drying at 20 °C and 60% RH with 3V DC voltage cyclic wetting	60 weeks	Yes	13/20	Propagation	Positive	Ahmed et al. [136]

OPC: ordinary Portland cement, FA: fly ash, SF: Silica fume.

6. Steel Bars in FRC Are Susceptible to Corrosion

Steel-fiber reinforcing bars cannot currently be used in the majority of civil engineering constructions, despite the fact that their use is increasing and they have already proven to be effective in structural reinforcement applications such as pre-cast pre-stressed beams and tunnel lining segments. It has been observed that fibers are used as secondary reinforcement in a variety of situations. According to Arya and Ofori-Darko [137], the influence of crack space and frequency of cracks on reinforcement corrosion has been investigated. The experiments were carried out with beam elements. The cracks on each beam were created by inserting shims into the concrete to produce a varying number of uniformly spaced and parallel-sided fractures. They were 40 mm in depth and varied in breadth depending on the amount of cracking present, with the cumulative crack width of each beam being 2.4 mm. The beams were maintained in a sealed atmosphere with a relative humidity of 90% and a temperature of 200 °C for the length of the experiment. NaCl solution of 3% was applied to the beams once every month for the first 28 days following casting in order to promote corrosion. Berrocal et al. [138] investigated the feasibility of employing a relatively new technology, distributed optical sensors based on optical frequency domain reflectometry, to detect cracks in concrete structures. Eight reinforced concrete beams were designed for this experiment. Two beams were used as control. Electrical strain foil gauges, optical fiber sensors, and DIC were used to measure the remaining six beams. Two of the beams were loaded monotonically to failure, while four were loaded cyclically. Based on the experiments, it was concluded that higher corrosion levels of bars were observed in plain concrete compared to fiber-reinforced concrete based on gravimetric measurements, and a more distributed corrosion pattern was observed in FRC. To determine the effect of two distinct forms of fiber reinforcement on the corrosion of traditional reinforcement, Kobayakawa et al. [139] carried out a series of experiments with two different types of fiber reinforcement, namely polyethylene (PE) fibers and steel fibers. Beam specimens made with these fibers, as well as specimens made with plain mortar and reinforced with a single steel bar, were subjected to wet–dry cycles in a solution containing 3% sodium chloride. When soaking was allowed for longer periods of time, the corrosion was further accelerated by applying a 3 V potential with an impressed current created by a DC power unit difference. Using current measurements and Faraday's law, it was predicted that polyethylene fibers would reduce corrosion.

Yoon et al. [140] studied the influence of differentloadlevels and sustainedloads on the corrosion of reinforcement in fracturedconcretemembers. To guarantee the stress transfer in structural applications, a sufficient bond betweenstrain-hardeningcementitious composites and steelrebarisnecessary. Due to the well-controlledsplitting cracks, the result shows that high-strength SHCC can bond muchbetterwithdeformedsteelrebarsthanordinaryconcrete and high-strength SHCC matrix (withoutfibers). A numericalapproach has been proposedwhich can beused for the design of reinforced SHCC elements and structures. Vidal et al. [141] studied the corrosion process of reinforced concrete beams that were exposed to salt fog for a period of 17 years. Every six months, the beams were tested for a range of parameters, including corrosion-induced fracture maps, chloride concentrations at the reinforcement level, corrosion distribution along the rebar, and mechanical performance. A full-scale beam element with longitudinal and shear reinforcement was used in this study. The beams were subjected to two different load levels, which was accomplished by the use of a three-point bending configuration. Following that, the beams were stored in a confined space and subjected to a salt fog comprising 35 g/L NaCl for many days. The fog was sprayed continuously for the first six years and then then sprayed on a weekly basis for the remaining six years of the experiment, while the temperature was kept constant at approximately 20 °C for the first nine years and then varied between 5 and 35 °C for the remaining nine years of the experiment. Based on experiment conducted, it can be concluded the corrosion of reinforcements was close to corrosion occurring in natural conditions with respect to distribution, corrosion type, and types of oxides produced. Liang Fan et al. [142] provide a new approach for calculating the mass loss of steel bars implanted in steel-fiber-reinforced concrete, to explore the effect of steel fibers on the mass loss of steel bars placed in concrete. The mass loss of the steel bar diminishes as the amount of fiber in the steel bar increases. The mass loss of steel bars implanted in steel-fiber-reinforced concrete was greatly overstated when Faraday's law was applied directly to the problem. This is probably true because the steel fibers only allocate a portion of the applied current [143,144]. The corrosion monitoring methods are listed in Table 3.

Table 3. Corrosion monitoring methods.

Nondestructive Methods	Principles	Merits	Demerits	Corrosion Evaluation	Specific Tools
Resistivity method [47]	RC resistance which current can simply switch connecting areas of anode and concrete cathode.	A simple, fast, compact, and cost-effective approach that can be used for regular inspection is available.	"Short circuit" and incorrect estimations might be caused by reinforcement in the test area.	Resistivity (Ω cm)	Current and potential electrode, volt units or resistance and insulation cable (working electrode)
Acoustic emission (AE) [96]	Acoustic emission can be characterized as a transient elastic wave created by the rapid release of energy inside a material.	It can recognize harmful defects that are hard to access with conventional nondestructive testing methods.	It might be slower than other nondestructive testing methods.	AE parameter	Transducer, preamplifier, filter, amplifier, and storage equipment

Table 3. *Cont.*

Nondestructive Methods	Principles	Merits	Demerits	Corrosion Evaluation	Specific Tools
Polarization resistance [105]	The estimation of the linear polarization resistance of steel in concrete is regularly used to assess the kinetics of steel dissolution inside a proven corrosion area.	Shorter time required for estimation and causes very little disturbances that do not interfere with the existing electrochemical procedures.	It requires some investment to get a total reaction because of electrical limit through the steel and concrete.	Corrosion current (Icorr) (A/cm^2)	Associating cable, security ring, counter-electrode (working electrode), and reference electrode
Infrared thermography (IRT) [133]	IR radiation emitted by concrete is converted into an electrical signal and used to create temperature maps on the surface of the ground.	Easy explanation of results without radiation, quick setup, portable and helpful method.	Corrosion damage is not quantifiable in any way.	Radiation power (E)	Multispectrum camera
Ultrasonic pulse velocity (UPV) [134]	When the pulse is introduced into the concrete by a transducer, it is subjected to multiple reflections at the limits of the different material stages inside the concrete.	Concrete testing equipment utilizing ultrasonic pulses gives faster and progressively exact results.	Fragment of ability and operator integrity is required. Subsequently, there is a requirement for trained and certified NDT personnel.	Pulse velocity (V)	Transducers (transmitter and receiver), amplifier, and oscillator
Galvanostatic pulse method (GPV) [138]	GPM corrosion evaluation depends on the existing measurement wanted to change the potential dissimilarity between the reinforcement and a standard reference electrode. The current is a result of electrons from the anodic and cathode sides in concrete.	Simple to learn, requiring a medium–low level of experience for equipment configuration and information collection.	Unstable estimations when resistance to concrete cover is high.	Potential resistance (Rct) ($k\Omega \cdot cm^2$)	Associating cable, security ring, counter-electrode (working electrode), and reference electrode
Open-circuit potential (OCP) monitoring [145]	The open-circuit voltage (OCV) refers to the entire electrochemical cell and the capacity of the open circuit to an electrode. This measure is intended to record the progress of the potential of the rest, e.g., when no current flow flows through the cell and a potential is applied to the electrode against a reference electrode or a potential contrast is applied to the cell.	The results are not equivalent contours, but a unique value that gives a sign of the state of the steel.	It requires a longer period of time and must be closed for a number of hours throughout the inspection.	Potential level (mV or V)	Potential electrode, voltmeter, and interfacing cable (working electrode)
Fiber Bragg grating (FBG) [146]	With an increase in steel reinforcement cross-section comes an increase in fiber stress, which is measured by FBG wavelength shifts.	Displays a linear response when measuring voltage, pressure, and temperature.	It is rather expensive to build and maintain.	Bragg wavelength (λB)	Bragg meter, Fiber optic sensor, and computer

7. Conclusions

Based on the literature review the following conclusions can be drawn:

The presence of fiber content in concrete can prevent the occurrence of cracking as well as result in a decrease in the width of cracked surfaces. Increases in the fiber volume of the concrete result in a change from shear to flexure failure modes, which results in an increase in the amount of time required for crack formation. Because of the relationship between crack size and permeability, fiber-reinforced concrete is more impermeable than conventional concrete in a cracked state. In uncracked concrete, the addition of fibers had no visible effect on the chloride diffusion coefficient, according to the experimental data that were collected and analyzed. Corrosion of the passive layer results in a lower resistivity of the concrete, and resistivity is critical in maintaining the integrity of the passive layer. Fibers may also reduce bond stress microcracks in uncracked samples, allowing for the same behavior to be observed. The presence of fibers increases the coefficient of chloride diffusion based on total chlorides. Fibers bind the chlorides and prevent their travel through the concrete. Fibers delay the start of corrosion in RC members as long as the applied load does not exceed a certain threshold value. The type of fibers and the volume of fibers used in RC members also impact the rate of corrosion. In spite of the fact that steel fibers can help reinforcing bars withstand corrosion, the impact of steel fibers on the corrosion rate and the risk of galvanic corrosion between steel fibers and reinforcing bars has not been specifically examined. Further research is being conducted to study the corrosion impact of steel fibers in addition to conventional reinforcement.

Funding: This research received no external funding.

Institutional Review Board Statement: Not applicable.

Conflicts of Interest: The authors declare no conflict of interest.

References

1. Hausmann, D.A. Steel corrosion in concrete—How does it occur? *Mater. Prot.* **1967**, *6*, 19–23.
2. Bentur, A. *Steel Corrosion in Concrete: Fundamentals and Civil Engineering Practice*; CRC Press: Boca Raton, FL, USA, 1997.
3. Hunkeler, F. Corrosion in Reinforced Concrete: Processes and Mechanisms. In *Woodhead Publishing Series in Civil and Structural Engineering*; Böhni, R.C.S., Ed.; Woodhead Publishing: Sawston, UK, 2005; pp. 1–45.
4. Tuutti, K. *Corrosion of Steel in Concrete*; Swedish Cement and Concrete Research Institute: Stockholm, Sweden, 1982.
5. Li, C.Q. Reliability Based Service Life Prediction of Corrosion Affected Concrete Structures. *J. Struct. Eng.* **2004**, *130*, 1570–1577. [CrossRef]
6. Ormellese, M.; Lazzari, L.; Goidanich, S.; Fumagalli, G.; Brenna, A. A study of organic substances as inhibitors for chloride-induced corrosion in concrete. *Corros. Sci.* **2009**, *51*, 2959–2968. [CrossRef]
7. Biczok, I. Concrete Corrosion and Concrete Protection. *Concr. Corros. Concr. Prot.* **2011**, *2*, 54–136.
8. Ahmad, S. Reinforcement corrosion in concrete structures, its monitoring and service life prediction—A review. *Cem. Concr. Compos.* **2003**, *25*, 459–471. [CrossRef]
9. Simčič, T.; Pejovnik, S.; De Schutter, G.; Bosiljkov, V.B. Chloride ion penetration into fly ash modified concrete during wetting–drying cycles. *Constr. Build. Mater.* **2015**, *93*, 1216–1223. [CrossRef]
10. Zhan, H.; Wittmann, F.H.; Zhao, T. Chloride Barrier for Concrete in Saline Environment Established by Water Repellent Treatment/DurchHydrophobierenhergestellteChloridschrankefürBeton in KontaktmitSalzwasser. *Restor. Build. Monum.* **2003**, *9*, 535–550. [CrossRef]
11. Liu, J.; Ou, G.; Qiu, Q.; Chen, X.; Hong, J.; Xing, F. Chloride transport and microstructure of concrete with/without fly ash under atmospheric chloride condition. *Constr. Build. Mater.* **2017**, *146*, 493–501. [CrossRef]
12. Medeiros, M.; Helene, P. Surface treatment of reinforced concrete in marine environment: Influence on chloride diffusion coefficient and capillary water absorption. *Constr. Build. Mater.* **2009**, *23*, 1476–1484. [CrossRef]
13. Medeiros, M.; Helene, P. Efficacy of surface hydrophobic agents in reducing water and chloride ion penetration in concrete. *Mater. Struct.* **2008**, *41*, 59–71. [CrossRef]
14. Win, P.P.; Watanabe, M.; Machida, A. Penetration profile of chloride ion in cracked reinforced concrete. *Cem. Concr. Res.* **2004**, *34*, 1073–1079. [CrossRef]
15. Conciatori, D.; Sadouki, H.; Brühwiler, E. Capillary suction and diffusion model for chloride ingress into concrete. *Cem. Concr. Res.* **2008**, *38*, 1401–1408. [CrossRef]
16. McCarter, W.J. Influence of Surface Finish on Sorptivity on Concrete. *J. Mater. Civ. Eng.* **1993**, *5*, 130–136. [CrossRef]
17. Ben Fraj, A.; Bonnet, S.; Khelidj, A. New approach for coupled chloride/moisture transport in non-saturated concrete with and without slag. *Constr. Build. Mater.* **2012**, *35*, 761–771. [CrossRef]
18. Xu, J.; Jiang, L.; Wang, J. Influence of detection methods on chloride threshold value for the corrosion of steel reinforcement. *Constr. Build. Mater.* **2009**, *23*, 1902–1908. [CrossRef]
19. Polder, R.B. Critical chloride content for reinforced concrete and its relationship to concrete resistivity. *Mater. Corros.* **2009**, *60*, 623–630. [CrossRef]
20. El-Dieb, A.S. Mechanical, durability and microstructural characteristics of ultra-high-strength self-compacting concrete incorporating steel fibers. *Mater. Des.* **2009**, *30*, 4286–4292. [CrossRef]

21. Barros, J. Steel fibre reinforced concrete: Material properties and structural applications. *FibrousCompos. Mater. Civ. Eng. Appl.* **2011**, 95–155. [CrossRef]
22. Kakooei, S.; Akil, H.M.; Dolati, A.; Rouhi, J. The corrosion investigation of rebar embedded in the fibers reinforced concrete. *Constr. Build. Mater.* **2012**, *35*, 564–570. [CrossRef]
23. Abbas, S.; Soliman, A.M.; Nehdi, M.L. Exploring mechanical and durability properties of ultra-high performance concrete incorporating various steel fiber lengths and dosages. *Constr. Build. Mater.* **2015**, *75*, 429–441. [CrossRef]
24. Yoo, D.-Y.; Shin, H.; Yang, J.-M.; Yoon, Y.-S. Material and bond properties of ultra high performance fiber reinforced concrete with micro steel fibers. *Compos. Part B Eng.* **2014**, *58*, 122–133. [CrossRef]
25. Simões, T.; Costa, H.; Dias-Da-Costa, D.; Julio, E. Influence of fibres on the mechanical behaviour of fibre reinforced concrete matrixes. *Constr. Build. Mater.* **2017**, *137*, 548–556. [CrossRef]
26. Romualdi, J.P.; Mandel, J.A. Tensile Strength of concrete Affected by UnigormlyDistributed and Closely Spaced Short Lengths of wire Reinforcement. *ACI J. Proc.* **1964**, *61*, 657–672. [CrossRef]
27. Furlan, S.; de Hanai, J.B. Shear behaviour of fiber reinforced concrete beams. *Cem. Concr. Compos.* **1997**, *19*, 359–366. [CrossRef]
28. Soroushian, P.; Elyamany, H.; Tlili, A.; Ostowari, K. Mixed-mode fracture properties of concrete reinforced with low volume fractions of steel and polypropylene fibers. *Cem. Concr. Compos.* **1998**, *20*, 67–78. [CrossRef]
29. Lim, D.; Oh, B. Experimental and theoretical investigation on the shear of steel fibre reinforced concrete beams. *Eng. Struct.* **1999**, *21*, 937–944. [CrossRef]
30. Bencardino, F.; Rizzuti, L.; Spadea, G.; Swamy, R. Experimental evaluation of fiber reinforced concrete fracture properties. *Compos. Part B Eng.* **2010**, *41*, 17–24. [CrossRef]
31. Qi, C.; Weiss, J.; Olek, J. Characterization of plastic shrinkage cracking in fiber reinforced concrete using image analysis and a modified Weibull function. *Mater. Struct.* **2003**, *36*, 386–395. [CrossRef]
32. Abrishami, H.H.; Mitchell, D. Influence of Steel Fibers on Tension Stiffening. *ACI Struct. J.* **1997**, *94*, 769–776. [CrossRef]
33. Swamy, R.; Mangat, P. A theory for the flexural strength of steel fiber reinforced concrete. *Cem. Concr. Res.* **1974**, *4*, 313–325. [CrossRef]
34. Kim, S.B.; Yi, N.H.; Kim, H.Y.; Kim, J.-H.J.; Song, Y.-C. Material and structural performance evaluation of recycled PET fiber reinforced concrete. *Cem. Concr. Compos.* **2010**, *32*, 232–240. [CrossRef]
35. Jalasutram, S.; Sahoo, D.R.; Matsagar, V. Experimental investigation of the mechanical properties of basalt fiber-reinforced concrete. *Struct. Concr.* **2017**, *18*, 292–302. [CrossRef]
36. Zia, A.; Ali, M. Behavior of fiber reinforced concrete for controlling the rate of cracking in canal-lining. *Constr. Build. Mater.* **2017**, *155*, 726–739. [CrossRef]
37. Li, V.C.; Matsumoto, T. Fatigue crack growth analysis of fiber reinforced concrete with effect of interfacial bond degradation. *Cem. Concr. Compos.* **1998**, *20*, 339–351. [CrossRef]
38. Ahmed, S.; Bukhari, I.A.; Siddiqui, J.I.; Qureshi, S.A. A study on properties of polypropylene fiber reinforced concrete. In Proceedings of the 31st Conference on Our World in Concrete and Structures, Singapore, 16–17 August 2006; pp. 63–72.
39. Barragan, B.; Gettu, R.; Agullo, L.; Zerbino, R. Shear failure of steel fiber-reinforced concrete based on push-off tests. *ACI Mater. J.* **2006**, *103*, 251.
40. Gopu, G.N.; Sofi, A. Electrical Waste Fibers Impact on Mechanical and Durability Properties of Concrete. *Civ. Eng. Archit.* **2021**, *9*, 1854–1868. [CrossRef]
41. Annamalai, S. Electrical conductivity of concrete. *ARPN J. Eng. Appl. Sci.* **2016**, *11*, 5979–5982.
42. Lataste, J.-F. *Electrical Resistivity for the Evaluation of Reinforced Concrete Structures*; Elsevier: Amsterdam, The Netherlands, 2010; pp. 243–275.
43. Saleem, M.; Shameem, M.; Hussain, S.; Maslehuddin, M. Effect of moisture, chloride and sulphate contamination on the electrical resistivity of Portland cement concrete. *Constr. Build. Mater.* **1996**, *10*, 209–214. [CrossRef]
44. Elsener, B.; Vennesland, Ø. Test methods for on site measurement of resistivity of concrete—A RILEM TC-154 technical recommendation. *Constr. Build. Mater.* **2001**, *15*, 125–131.
45. Lakshminarayanan, V.; Ramesh, P.S.; Rajagopalan, S.R. A new technique for the measurement of the electrical resistivity of concrete. *Mag. Concr. Res.* **1992**, *44*, 47–52. [CrossRef]
46. Sbartaï, Z.; Laurens, S.; Rhazi, J.; Balayssac, J.; Arliguie, G. Using radar direct wave for concrete condition assessment: Correlation with electrical resistivity. *J. Appl. Geophys.* **2007**, *62*, 361–374. [CrossRef]
47. Sengul, O. Use of electrical resistivity as an indicator for durability. *Constr. Build. Mater.* **2014**, *73*, 434–441. [CrossRef]
48. Ghods, P.; Alizadeh, A.R.; Salehi, M. Electrical Resistivity of Concrete. 2015, pp. 41–46. Available online: https://www.giatecscientific.com/wp-content/uploads/2015/05/Concrete_Electrical_Resistivity.pdf (accessed on 1 May 2015).
49. Cheytani, M.; Chan, S. The applicability of the Wenner method for resistivity measurement of concrete in atmospheric conditions. *Case Stud. Constr. Mater.* **2021**, *15*, e00663. [CrossRef]
50. Sun, W.; Mu, R.; Luo, X.; Miao, C. Effect of chloride salt, freeze-thaw cycling and externally applied load on the performance of the concrete. *Cem. Concr. Res.* **2002**, *32*, 1859–1864. [CrossRef]
51. Cheng, Y.; Zhang, Y.; Wu, C.; Jiao, Y. Experimental and Simulation Study on Diffusion Behavior of Chloride Ion in Cracking Concrete and Reinforcement Corrosion. *Adv. Mater. Sci. Eng.* **2018**, *2018*, 8475384. [CrossRef]

52. Tammo, K.; Lundgren, K.; Thelandersson, S.; Högskola, T. Chalmers Publication Library Crack Widths Close to the Reinforcement Crack Widths Close to the Reinforcement. Available online: http://publications.lib.chalmers.se/publication/54301 (accessed on 16 November 2021).
53. Tao, Y.; Gou, Z.; Yu, Z.; Fu, J.; Chen, X. The challenge of creating age-friendly indoor environments in a high-density city: Case study of Hong Kong's care and attention homes. *J. Build. Eng.* **2020**, *30*, 101280. [CrossRef]
54. Kobayashi, K.; Le Ahn, D.; Rokugo, K. Effects of crack properties and water-cement ratio on the chloride proofing performance of cracked SHCC suffering from chloride attack. *Cem. Concr. Compos.* **2016**, *69*, 18–27. [CrossRef]
55. Jaffer, S.; Hansson, C. The influence of cracks on chloride-induced corrosion of steel in ordinary Portland cement and high performance concretes subjected to different loading conditions. *Corros. Sci.* **2008**, *50*, 3343–3355. [CrossRef]
56. Marsavina, L.; Audenaert, K.; De Schutter, G.; Faur, N.; Marsavina, D. Experimental and numerical determination of the chloride penetration in cracked concrete. *Constr. Build. Mater.* **2009**, *23*, 264–274. [CrossRef]
57. Park, S.-S.; Kwon, S.-J.; Jung, S.H. Analysis technique for chloride penetration in cracked concrete using equivalent diffusion and permeation. *Constr. Build. Mater.* **2012**, *29*, 183–192. [CrossRef]
58. Kim, Y.Y.; Kim, J.-M.; Bang, J.-W.; Kwon, S.-J. Effect of cover depth, w/c ratio, and crack width on half cell potential in cracked concrete exposed to salt sprayed condition. *Constr. Build. Mater.* **2014**, *54*, 636–645. [CrossRef]
59. Ye, H.; Tian, Y.; Jin, N.; Jin, X.; Fu, C. Influence of cracking on chloride diffusivity and moisture influential depth in concrete subjected to simulated environmental conditions. *Constr. Build. Mater.* **2013**, *47*, 66–79. [CrossRef]
60. Yu, L.; Francois, R.; Dang, V.H.; L'Hostis, V.; Gagné, R. Development of chloride-induced corrosion in pre-cracked RC beams under sustained loading: Effect of load-induced cracks, concrete cover, and exposure conditions. *Cem. Concr. Res.* **2015**, *67*, 246–258. [CrossRef]
61. Otieno, M.; Beushausen, H.; Alexander, M. Chloride-induced corrosion of steel in cracked concrete—Part I: Experimental studies under accelerated and natural marine environments. *Cem. Concr. Res.* **2016**, *79*, 373–385. [CrossRef]
62. Wang, Y.; Cao, Y.; Zhang, P.; Ma, Y.; Zhao, T.; Wang, H.; Zhang, Z. Water absorption and chloride diffusivity of concrete under the coupling effect of uniaxial compressive load and freeze-thaw cycles. *Constr. Build. Mater.* **2019**, *209*, 566–576. [CrossRef]
63. Guo, Y.; Hu, X.; Lv, J. Experimental study on the resistance of basalt fibre-reinforced concrete to chloride penetration. *Constr. Build. Mater.* **2019**, *223*, 142–155. [CrossRef]
64. *ASTM G109-07*; Standard Test Method for Determining the Effects of Chemical Admixtures on the Corrosion of Embedded Steel Reinforcement in Concrete Exposed to Chloride Environments. ASTM International: West Conshohocken, PA, USA, 2000.
65. Andrade, C.; Prieto, M.; Tanner, P.; Tavares, F.; D'Andrea, R. Testing and modelling chloride penetration into concrete. *Constr. Build. Mater.* **2013**, *39*, 9–18. [CrossRef]
66. Zhang, W.; François, R.; Yu, L. Influence of load-induced cracks coupled or not with top-casting-induced defects on the corrosion of the longitudinal tensile reinforcement of naturally corroded beams exposed to chloride environment under sustained loading. *Cem. Concr. Res.* **2020**, *129*, 105972. [CrossRef]
67. Güneyisi, E.; Gesoğlu, M.; Karaboğa, F.; Mermerdaş, K. Corrosion behavior of reinforcing steel embedded in chloride contaminated concretes with and without metakaolin. *Compos. Part B Eng.* **2013**, *45*, 1288–1295. [CrossRef]
68. Jing, L.; Yin, S.; Lv, H. Bonding Behavior of Textile Reinforced Concrete (TRC)-Confined Concrete and Reinforcement under Chloride Erosion Environment. *KSCE J. Civ. Eng.* **2020**, *24*, 826–834. [CrossRef]
69. Daghe, L.E.; Legione, D. Covariance structure analysis of health-related indicators in the elderly at home with a focus on subjective health. *J-GLOBAL* **1987**, *17*, 105–120. (In Japanese)
70. El Maaddawy, T.; Chahrour, A.; Soudki, K. Effect of Fiber-Reinforced Polymer Wraps on Corrosion Activity and Concrete Cracking in Chloride-Contaminated Concrete Cylinders. *J. Compos. Constr.* **2006**, *10*, 139–147. [CrossRef]
71. Soudki, K.; El-Salakawy, E.; Craig, B. Behavior of CFRP Strengthened Reinforced Concrete Beams in Corrosive Environment. *J. Compos. Constr.* **2007**, *11*, 291–298. [CrossRef]
72. Banthia, N. Durability enhancements in concrete with fiber reinforcement. In Proceedings of the Conference on Sustainable Construction Materials and Technologies, Coventry, UK, 11–13 June 2007; pp. 209–219.
73. Abbas, S.; Soliman, A.M.; Nehdi, M.L. Chloride Ion Penetration in RC and SFRC Precast Tunnel Lining Segments. *ACI Mater. J.* **2014**, *111*, 613–622. [CrossRef]
74. Corinaldesi, V.; Moriconi, G. Mechanical and thermal evaluation of Ultra High Performance Fiber Reinforced Concretes for engineering applications. *Constr. Build. Mater.* **2012**, *26*, 289–294. [CrossRef]
75. Šavija, B.; Luković, M.; Hosseini, S.A.S.; Pacheco, J.; Schlangen, E. Corrosion induced cover cracking studied by X-ray computed tomography, nanoindentation, and energy dispersive X-ray spectrometry (EDS). *Mater. Struct.* **2015**, *48*, 2043–2062. [CrossRef]
76. Luković, M.; Šavija, B.; Ye, G.; Schlangen, E.; Van Breugel, K. Failure Modes in Concrete Repair Systems due to Ongoing Corrosion. *Adv. Mater. Sci. Eng.* **2017**, *2017*, 9649187. [CrossRef]
77. Michel, A.; Solgaard, A.; Pease, B.J.; Geiker, M.R.; Stang, H.; Olesen, J.F. Experimental investigation of the relation between damage at the concrete-steel interface and initiation of reinforcement corrosion in plain and fibre reinforced concrete. *Corros. Sci.* **2013**, *77*, 308–321. [CrossRef]
78. Sahmaran, M.; Li, M.; Li, V.C. Transport Properties of Engineered Cementitious Composites under Chloride Exposure. *ACI Mater. J.* **2007**, *104*, 604–611. [CrossRef]

79. Şahmaran, M.; Li, V.C. Durability properties of micro-cracked ECC containing high volumes fly ash. *Cem. Concr. Res.* **2009**, *39*, 1033–1043. [CrossRef]
80. Bhargava, A.; Banthia, N. Permeability of concrete with fiber reinforcement and service life predictions. *Mater. Struct.* **2007**, *41*, 363–372. [CrossRef]
81. Liu, J.; Jia, Y.; Wang, J. Calculation of chloride ion diffusion in glass and polypropylene fiber-reinforced concrete. *Constr. Build. Mater.* **2019**, *215*, 875–885. [CrossRef]
82. Söylev, T.A.; Özturan, T. Durability, physical and mechanical properties of fiber-reinforced concretes at low-volume fraction. *Constr. Build. Mater.* **2014**, *73*, 67–75. [CrossRef]
83. Akhavan, A.; Rajabipour, F. Evaluating ion diffusivity of cracked cement paste using electrical impedance spectroscopy. *Mater. Struct.* **2012**, *46*, 697–708. [CrossRef]
84. Ramli, M.; Kwan, W.H.; Abas, N.F. Strength and durability of coconut-fiber-reinforced concrete in aggressive environments. *Constr. Build. Mater.* **2013**, *38*, 554–566. [CrossRef]
85. Berrocal, C.G.; Löfgren, I.; Lundgren, K.; Tang, L. Corrosion initiation in cracked fibre reinforced concrete: Influence of crack width, fibre type and loading conditions. *Corros. Sci.* **2015**, *98*, 128–139. [CrossRef]
86. Niu, D.; Huang, D.; Fu, Q. Experimental investigation on compressive strength and chloride permeability of fiber-reinforced concrete with basalt-polypropylene fibers. *Adv. Struct. Eng.* **2019**, *22*, 2278–2288. [CrossRef]
87. Corrosion-Induced Cracking Time in Steel Fiber-Reinforced Concrete: Experiment and Finite Element Method. *ACI Mater. J.* **2020**, *117*, 3–12. [CrossRef]
88. Örnek, C.; Leygraf, C.; Pan, J. Passive film characterisation of duplex stainless steel using scanning Kelvin probe force microscopy in combination with electrochemical measurements. *NPJ Mater. Degrad.* **2019**, *3*, 8. [CrossRef]
89. Ann, K.Y.; Song, H.-W. Chloride threshold level for corrosion of steel in concrete. *Corros. Sci.* **2007**, *49*, 4113–4133. [CrossRef]
90. Berrocal, C.G.; Fernandez, I.; Lundgren, K.; Lofgren, I. Corrosion-induced cracking and bond behaviour of corroded reinforcement bars in SFRC. *Compos. Part B Eng.* **2017**, *113*, 123–137. [CrossRef]
91. Stefanoni, M.; Angst, U.; Elsener, B. Corrosion Challenges and Opportunities in Digital Fabrication of Reinforced Concrete. In *RILEM International Conference on Concrete and Digital Fabrication*; Springer: Amsterdam, The Netherlands, 2019; pp. 225–233. [CrossRef]
92. Fang, C.; Lundgren, K.; Chen, L.; Zhu, C. Corrosion influence on bond in reinforced concrete. *Cem. Concr. Res.* **2004**, *34*, 2159–2167. [CrossRef]
93. Šavija, B.; Luković, M. Carbonation of cement paste: Understanding, challenges, and opportunities. *Constr. Build. Mater.* **2016**, *117*, 285–301. [CrossRef]
94. Mangat, P.; Gurusamy, K. Corrosion resistance of steel fibres in concrete under marine exposure. *Cem. Concr. Res.* **1988**, *18*, 44–54. [CrossRef]
95. Zhou, J.; Chen, X.; Chen, S. Effect of different environments on bond strength of glass fiber-reinforced polymer and steel reinforcing bars. *KSCE J. Civ. Eng.* **2012**, *16*, 994–1002. [CrossRef]
96. Neale, K.W.; Labossière, P.; Thériault, M. FRPs for Strengthening and Rehabilitation: Durability Issues. In *Composites in Construction*; American Society of Civil Engineers: Reston, VA, USA, 2001; pp. 102–109.
97. Yu, A.-P.; Naqvi, M.W.; Hu, L.-B.; Zhao, Y.-L. An experimental study of corrosion damage distribution of steel bars in reinforced concrete using acoustic emission technique. *Constr. Build. Mater.* **2020**, *254*, 119256. [CrossRef]
98. Roussel, N.; Cussigh, F. Distinct-layer casting of SCC: The mechanical consequences of thixotropy. *Cem. Concr. Res.* **2008**, *38*, 624–632. [CrossRef]
99. Wangler, T.; Lloret, E.; Reiter, L.; Hack, N.; Gramazio, F.; Kohler, M.; Bernhard, M.; Dillenburger, B.; Buchli, J.; Roussel, N.; et al. Digital Concrete: Opportunities and Challenges. *RILEM Tech. Lett.* **2016**, *1*, 67–75. [CrossRef]
100. Kim, H.-Y.; Park, Y.-H.; You, Y.-J.; Moon, C.-K. Short-term durability test for GFRP rods under various environmental conditions. *Compos. Struct.* **2008**, *83*, 37–47. [CrossRef]
101. Ding, Y.; Ning, X.; Zhang, Y.; Pacheco-Torgal, F.; Aguiar, J. Fibres for enhancing of the bond capacity between GFRP rebar and concrete. *Constr. Build. Mater.* **2014**, *51*, 303–312. [CrossRef]
102. Liu, T.-Y.; Zhang, P.; Li, Q.-F.; Hu, S.-W.; Ling, Y.-F. Durability Assessment of PVA Fiber-Reinforced Cementitious Composite Containing Nano-SiO_2 Using Adaptive Neuro-Fuzzy Inference System. *Crystals* **2020**, *10*, 347. [CrossRef]
103. Behnood, A.; Van Tittelboom, K.; De Belie, N. Methods for measuring pH in concrete: A review. *Constr. Build. Mater.* **2016**, *105*, 176–188. [CrossRef]
104. Almusallam, A.A.; Al-Gahtani, A.S.; Aziz, A.R. Rasheeduzzafar Effect of reinforcement corrosion on bond strength. *Constr. Build. Mater.* **1996**, *10*, 123–129. [CrossRef]
105. Zhang, R.; Castel, A.; Francois, R. Concrete cover cracking with reinforcement corrosion of RC beam during chloride-induced corrosion process. *Cem. Concr. Res.* **2010**, *40*, 415–425. [CrossRef]
106. Rivera-Corral, J.; Fajardo, G.; Arliguie, G.; Orozco-Cruz, R.; Deby, F.; Valdez, P. Corrosion behavior of steel reinforcement bars embedded in concrete exposed to chlorides: Effect of surface finish. *Constr. Build. Mater.* **2017**, *147*, 815–826. [CrossRef]
107. Jia, D.; Guo, Q.; Mao, J.; Lv, J.; Yang, Z. Durability of glass fibre-reinforced polymer (GFRP) bars embedded in concrete under various environments. I: Experiments and analysis. *Compos. Struct.* **2020**, *234*, 111687. [CrossRef]
108. Perna, I. Microscopic study of the concrete/geopolymer coating interface. *Ceram. Silik.* **2019**, *64*, 68–74. [CrossRef]

109. Granju, J.-L.; Balouch, S.U. Corrosion of steel fibre reinforced concrete from the cracks. *Cem. Concr. Res.* **2005**, *35*, 572–577. [CrossRef]
110. Fu, C.; Zhou, K.; Ling, Y.; Jin, X.; Fang, D.; Zhou, J. Chloride transport behavior in bending-shear section of reinforced concrete beam under combined effect of load and environment. *Constr. Build. Mater.* **2020**, *257*, 119533. [CrossRef]
111. Murad, Y.; Tarawneh, A.; Arar, F.; Al-Zu'bi, A.; Al-Ghwairi, A.; Al-Jaafreh, A.; Tarawneh, M. Flexural strength prediction for concrete beams reinforced with FRP bars using gene expression programming. *Structures* **2021**, *33*, 3163–3172. [CrossRef]
112. Balouch, S.; Forth, J.; Granju, J.-L. Surface corrosion of steel fibre reinforced concrete. *Cem. Concr. Res.* **2010**, *40*, 410–414. [CrossRef]
113. Nkurunziza, G.; Benmokrane, B.; Debaiky, A.S.; Masmoudi, R. Effect of sustained load environment on long-term tensile properties of glass fiber-reinforcing polymer reinforcing bars. *ACI Mater. J.* **2005**, *102*, 615–621.
114. Shepherd, D.A.; Kotan, E.; Dehn, F. Plastic concrete for cut-off walls: A review. *Constr. Build. Mater.* **2020**, *255*, 119248. [CrossRef]
115. Stefanoni, M.; Angst, U.; Elsener, B. Corrosion rate of carbon steel in carbonated concrete—A critical review. *Cem. Concr. Res.* **2018**, *103*, 35–48. [CrossRef]
116. Chen, Y.; Davalos, J.F.; Ray, I. Durability Prediction for GFRP Reinforcing Bars Using Short-Term Data of Accelerated Aging Tests. *J. Compos. Constr.* **2006**, *10*, 279–286. [CrossRef]
117. Dai, J.-G.; Yokota, H.; Iwanami, M.; Kato, E. Experimental Investigation of the Influence of Moisture on the Bond Behavior of FRP to Concrete Interfaces. *J. Compos. Constr.* **2010**, *14*, 834–844. [CrossRef]
118. Jiradilok, P.; Wang, Y.; Nagai, K.; Matsumoto, K. Development of discrete meso-scale bond model for corrosion damage at steel-concrete interface based on tests with/without concrete damage. *Constr. Build. Mater.* **2020**, *236*, 117615. [CrossRef]
119. Benmokrane, B.; Tighiouart, B.; Chaallal, O. Bond strength and load distribution of composite GFRP reinforcing bars in concrete. *ACI Mater. J.* **1996**, *93*, 246–253.
120. Suescún, L.; Sanchez, E.; Gómez, M.; Garcia-Arias, F.L.; NúñezZarantes, V.M. *Producción de Plantasgenéticamentepuras de Uchuva*; Editorial Kimpres Ltd.: Kennedy, Colombia, 2011.
121. Pakravan, H.R.; Latifi, M.; Jamshidi, M. Hybrid short fiber reinforcement system in concrete: A review. *Constr. Build. Mater.* **2017**, *142*, 280–294. [CrossRef]
122. Malvar, L.J. Tensile and bond properties of GFRP reinforcing bars. *ACI Mater. J.* **1995**, *92*, 276–285.
123. Fan, X.; Guan, X.; Ma, J.; Ai, H. Kinetics and corrosion products of aqueous nitrate reduction by iron powder without reaction conditions control. *J. Environ. Sci.* **2009**, *21*, 1028–1035. [CrossRef]
124. Kamal, A.S.M.; Boulfiza, M. Durability of GFRP Rebars in Simulated Concrete Solutions under Accelerated Aging Conditions. *J. Compos. Constr.* **2011**, *15*, 473–481. [CrossRef]
125. Barneyback, R.; Diamond, S. Expression and analysis of pore fluids from hardened cement pastes and mortars. *Cem. Concr. Res.* **1981**, *11*, 279–285. [CrossRef]
126. Stefanoni, M.; Angst, U.; Elsener, B. Local electrochemistry of reinforcement steel—Distribution of open circuit and pitting potentials on steels with different surface condition. *Corros. Sci.* **2015**, *98*, 610–618. [CrossRef]
127. Gartner, E.; Hirao, H. A review of alternative approaches to the reduction of CO_2 emissions associated with the manufacture of the binder phase in concrete. *Cem. Concr. Res.* **2015**, *78*, 126–142. [CrossRef]
128. Mangat, P.S.; Gurusamy, K. Permissible crack widths in steel fibre reinforced marine concrete. *Mater. Struct.* **1987**, *20*, 338–347. [CrossRef]
129. Nemegeer, D.; Vanbrabant, J.; Stang, H. Brite Euram program on steel fibre concrete subtask: DurabilityCorrosion resistance of cracked fibre reinforced concrete. In *International RILEM Workshop on Test and Design Methods for Steelfibre Reinforced Concrete*; RILEM Publications SARL: Paris, France, 2003; pp. 47–66.
130. Kim, D.J.; Wille, K.; Naaman, A.E.; El-Tawil, S. Strength Dependent Tensile Behavior of Strain Hardening Fiber Reinforced Concrete. *RILEM Bookser.* **2012**, *2*, 3–10. [CrossRef]
131. Mihashi, H.; Ahmed, S.F.U.; Kobayakawa, A. Corrosion of Reinforcing Steel in Fiber Reinforced Cementitious Composites. *J. Adv. Concr. Technol.* **2011**, *9*, 159–167. [CrossRef]
132. Parra-Montesinos, G.J.; Reinhardt, H.W.; Naaman, A.E. *High Performance Fiber Reinforced Cement Composites 6*; Springer: Berlin/Heidelberg, Germany, 2012.
133. Angst, U.M.; Geiker, M.R.; Michel, A.; Gehlen, C.; Wong, H.; Isgor, O.B.; Elsener, B.; Hansson, C.M.; François, R.; Hornbostel, K.; et al. The steel—Concrete interface. *Mater. Struct.* **2017**, *50*, 143. [CrossRef]
134. Liu, P.; Hu, Y.; Chen, Y.; Geng, B.; Xu, D. Investigation of novel embedded piezoelectric ultrasonic transducers on crack and corrosion monitoring of steel bar. *Constr. Build. Mater.* **2020**, *235*, 117495. [CrossRef]
135. Farhan, N.A.; Sheikh, M.N.; Hadi, M.N. Experimental Investigation on the Effect of Corrosion on the Bond between Reinforcing Steel Bars and Fibre Reinforced Geopolymer Concrete. *Structure* **2018**, *14*, 251–261. [CrossRef]
136. Harajli, M.H. Bond Stress—Slip Model for Steel Bars in Unconfined or Steel, FRC, or FRP Confined Concrete under Cyclic Loading. *J. Struct. Eng.* **2009**, *135*, 509–518. [CrossRef]
137. Pyo, S.; Koh, T.; Tafesse, M.; Kim, H.-K. Chloride-induced corrosion of steel fiber near the surface of ultra-high performance concrete and its effect on flexural behavior with various thickness. *Constr. Build. Mater.* **2019**, *224*, 206–213. [CrossRef]
138. Hou, L.; Li, Y.; Sun, J.; Zhang, S.H.; Wei, H.; Wei, Y. Enhancement corrosion resistance of Mg Al layered double hydroxides films by anion-exchange mechanism on magnesium alloys. *Appl. Surf. Sci.* **2019**, *487*, 101–108. [CrossRef]

139. Ramanathan, S.; Benzecry, V.; Suraneni, P.; Nanni, A. Condition assessment of concrete and glass fiber reinforced polymer (GFRP) rebar after 18 years of service life. *Case Stud. Constr. Mater.* **2021**, *14*, e00494. [CrossRef]
140. Maalej, M.; Chhoa, C.; Quek, S.T. Effect of cracking, corrosion and repair on the frequency response of RC beams. *Constr. Build. Mater.* **2010**, *24*, 719–731. [CrossRef]
141. El Refai, A.; Ammar, M.-A.; Masmoudi, R. Bond Performance of Basalt Fiber-Reinforced Polymer Bars to Concrete. *J. Compos. Constr.* **2015**, *19*, 04014050. [CrossRef]
142. Arya, C.; Ofori-Darko, F. Influence of crack frequency on reinforcement corrosion in concrete. *Cem. Concr. Res.* **1996**, *26*, 345–353. [CrossRef]
143. Berrocal, C.G.; Löfgren, I.; Lundgren, K. The effect of fibres on steel bar corrosion and flexural behaviour of corroded RC beams. *Eng. Struct.* **2018**, *163*, 409–425. [CrossRef]
144. Morcous, G.; Cho, Y.; El-Safty, A.; Chen, G. Structural behavior of FRP sandwich panels for bridge decks. *KSCE J. Civ. Eng.* **2010**, *14*, 879–888. [CrossRef]
145. Kim, H.-Y.; Park, Y.-H.; You, Y.-J.; Moon, C.-K. Durability of GFRP composite exposed to various environmental conditions. *KSCE J. Civ. Eng.* **2006**, *10*, 291–295. [CrossRef]
146. Chen, Y.; Yu, J.; Younas, H.; Leung, C.K. Experimental and numerical investigation on bond between steel rebar and high-strength Strain-Hardening Cementitious Composite (SHCC) under direct tension. *Cem. Concr. Compos.* **2020**, *112*, 103666. [CrossRef]